Probing Conformational Plasticity of the Activation Domain of Trypsin: The Role of Glycine Hinges †

ARTICLE *in* BIOCHEMISTRY · MARCH 2008

Impact Factor: 3.02 · DOI: 10.1021/bi701454e · Source: PubMed

7 AUTHORS, INCLUDING:

Laszlo Szilagyi
Eötvös Loránd University
74 PUBLICATIONS **1,695** CITATIONS

SEE PROFILE

Andras Malnasi
Eötvös Loránd University
68 PUBLICATIONS **1,336** CITATIONS

SEE PROFILE

Probing Conformational Plasticity of the Activation Domain of Trypsin: The Role of Glycine Hinges†

Linda Gombos, József Kardos, András Patthy, Péter Medveczky, László Szilágyi, András Málnási-Csizmadia, and László Gráf*

Department of Biochemistry, Eötvös Loránd University, Pázmány Péter sétány 1/C, H-1117 Budapest, Hungary

Received July 24, 2007; Revised Manuscript Received November 30, 2007

ABSTRACT: Trypsin-like serine proteases play essential roles in diverse physiological processes such as hemostasis, apoptosis, signal transduction, reproduction, immune response, matrix remodeling, development, and differentiation. All of these proteases share an intriguing activation mechanism that involves the transition of an unfolded domain (activation domain) of the zymogen to a folded one in the active enzyme. During this conformational change, activation domain segments move around highly conserved glycine hinges. In the present study, hinge glycines were replaced by alanine residues *via* site directed mutagenesis. The effects of these mutations on the interconversion of the zymogen-like and active conformations as well as on catalytic activity were studied. Mutant trypsins showed zymogen-like structures to varying extents characterized by increased flexibility of some activation domain segments, a more accessible N-terminus and a deformed substrate binding site. Our results suggest that the trypsinogen to trypsin transition is hindered by the mutations, which results in a shift of the equilibrium between the inactive zymogen-like and active enzyme conformations toward the inactive state. Our data also showed, however, that the inactive conformations of the various mutants differ from each other. Binding of substrate analogues shifted the conformational equilibrium toward the active enzyme since inhibited forms of the trypsin mutants showed similar structural features as the wild-type enzyme. The catalytic activity of the mutants correlated with the proper conformation of the active site, which could be supported by varying conformations of the N-terminus and the autolysis loop. Transient kinetic measurements confirmed the existence of an inactive to active conformational transition occurring prior to substrate binding.

Trypsin can be seen as a model of the serine endopeptidases of family S1, the most abundant proteases in nature (*1*, *2*). Trypsin-like serine proteases play essential roles in diverse physiological processes such as hemostasis, apoptosis, signal transduction, reproduction, immune response, matrix remodeling, development, and differentiation. All of these proteases have evolved to specialized functions from a common ancestor with tryptic specificity and a digestive role (*3*, *4*). Moreover, a large combination of structural and biochemical data makes trypsin an ideal system to explore general features of protein folding and function. Proteolytic enzymes are synthesized as inactive precursors (or zymogens) to enable spatial and temporal regulation of proteolytic activity and to prevent uncontrolled proteolytic degradation (*5*). Zymogens generally contain N-terminal extensions, and proteolytic removal of this peptide converts the zymogen to the active enzyme. In most cases, prosegments exert their inhibitory action through sterically blocking the active site and thereby preventing substrate binding. However, the propeptide of trypsin-like serine proteases stabilizes the inactive zymogen conformation, and cleavage of this peptide segment triggers a folding process. Approximately 85% of the structures of the zymogen and active trypsin including the catalytic residues are organized identically. The remaining 15% of the molecule (activation domain), consisting of the N-terminus to residue 19 and three loop segments (residues 142−152, 184−193, and 216−223), undergoes a series of concerted conformational changes following activation (*6*, *7*). This region, which includes the substrate binding site and the oxyanion hole, is incompletely folded in the zymogen, resulting in the inactivity of trypsinogen. In the active enzyme, the activation domain becomes ordered and forms a relatively closed domain with mostly internal contacts stabilized by a salt bridge between the newly liberated Ile16 N-terminus and the Asp194 carboxylate. Strong binding of an inhibitor, e.g., bovine pancreatic trypsin inhibitor, can also induce a conformation in trypsinogen that closely resembles the structure of trypsin with a rigid, correctly designed active site and Ile16 pocket, although there is no free Ile16 N-terminus available (*8*, *9*). The structural transition can also be induced from the other site: titration or covalent modification of the Ile16 N-terminus of trypsin leads to inactivation, demonstrating an allosteric linkage between the Ile16 N-terminus and the active site (*10*−*12*). These observations suggest that both trypsinogen and trypsin can exist in two conformations: an inactive, zymogen-like and an active, trypsin-like conformation. These two conformations

† This work was supported by Hungarian Scientific Research Fund Grants OTKA TS49812 and T047154 (to L. Gráf) and K68464 (to J.K.) and by a National Office for Research and Technology grant RET 14/2005 (to A.M.-C.). L. Gombos was supported by a Deák Ferenc fellowship. J.K. was supported by a Bolyai János fellowship.

* Corresponding author. Phone: +36-1-3812171. Fax: +36-1-3812172. E-mail: graf@elte.hu.

10.1021/bi701454e CCC: $40.75
Published on Web 01/15/2008

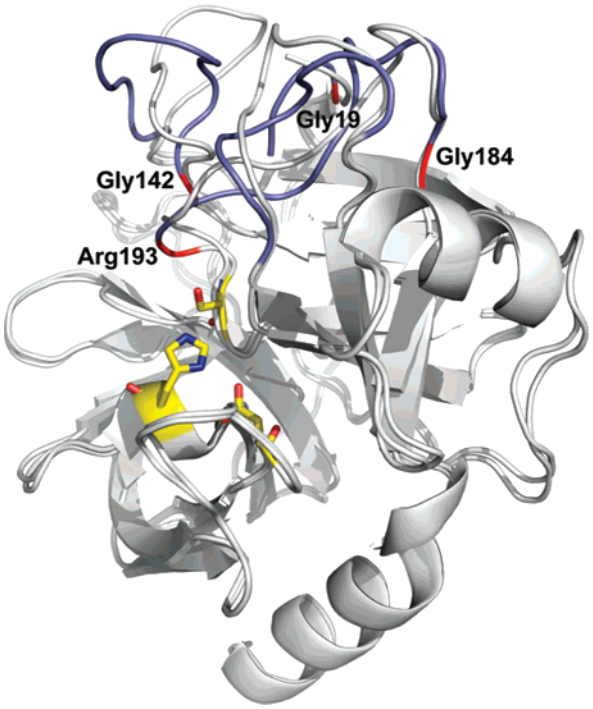

FIGURE 1: The aligned three-dimensional structures of human trypsin 4 and bovine trypsinogen. The activation domain segments of human trypsin 4 are shaded in blue, and the catalytic triad is shown in yellow. The hinge positions 19, 142, 184 and 193 are highlighted in red. The figure was prepared using the structures 1H4W and 1TGN and the program PyMOL (DeLano Scientific) (*21*).

are in equilibrium, with $K_{eq} = 10^7$ in favor of the inactive conformation for trypsinogen but with $K_{eq} = 10^2$ in favor of the active conformation for trypsin (*13*).

It is remarkable that in five of the seven positions that join activation domain segments to the ordered molecular segments a glycine residue is located. This observation is consistent with the fact that the presence of glycines facilitates flexibility of the protein backbone as the absence of a side chain results in a lower torsion barrier for the rotation around φ and ψ bonds. Indeed, the results of molecular dynamics simulations show that these glycines undergo larger dihedral angle transitions during the activation process than surrounding residues (*14*−*16*). This suggests that the glycine residues act as hinges for the conformational change of activation domain segments during activation. Hinge glycine residues are highly conserved in serine proteases; moreover, they are invariant even in proteins with a serine protease fold but lacking protease activity, e.g., hepatocyte growth factor (*17*). This indicates a predominant role of these glycines in the overall protein architecture. A few exceptions exist for position 193, which not only plays a role in the conformational transition accompanying activation but is also part of the oxyanion hole and occupies the S2′ subsite of the substrate binding cleft. One example is human trypsinogen 4, in which Gly193 is replaced by an arginine residue (Figure 1) (*18*−*20*). Recently, we studied the effect of the conformational freedom around this hinge on the activation process of human trypsin 4 and found that the rate of the conformational transition negatively correlates with the size of the side chain of the amino acid at position 193 (*22*). We also demonstrated that replacement of the conserved Gly193 by an amino acid with a bulky side chain greatly affects the hydrolysis of 4-methylumbelliferyl 4-guanidinobenzoate (MUGB[1]) substrate analogue (*23*). Thermodynamic analysis of the acylation step revealed that significantly more extended structural rearrangements occur at the formation of the first tetrahedral intermediate in wild-type human trypsin 4 compared to the R193G variant. These results suggest, as it has been proposed earlier (*24*), that the catalytic mechanism of serine proteases may involve structural movements of some parts of the activation domain. The goal of the present work was to study the effects of perturbation of hinge flexibility of the activation domain on the zymogen/active enzyme interconversion and catalytic properties of trypsin. We replaced hinge glycines by alanine residues *via* site-directed mutagenesis. These mutations had no effect on the stability and correct fold of the zymogen form; however, they caused structural perturbation in the activation domain of the activated enzyme. The structural effects of these mutations were studied by systematically probing characteristics of the zymogen form, i.e., increased flexibility of the autolysis loop, a free N-terminus, and a deformed substrate binding site. Dependent on the site of the mutation, however, these structural changes are different and differentially affect the conformational equilibrium between the various inactive and the active forms of the mutant enzyme. Consequently, the catalytic activities of the mutants are reduced to different extents and this reduction correlates with deformation of the active site.

EXPERIMENTAL PROCEDURES

Construction of Trypsinogen Mutants. Construction of expression plasmids for wild-type human trypsin 4 and engineering of the R193G and R193A mutants were described previously (*22*, *23*, *25*). Mutation G19A was introduced into the R193G human trypsin 4 mutant by PCR using the following forward primer (mutated nucleotides are shown in boldface type) G19A 5′-GCTGAAGCTTTCCCCGTTGACGATGATGACAAGATTGTTGGGG**C**CTAC ACCTGTGAG-3′ (Invitrogen), and the mutations G142A and G184A were introduced by the megaprimer mutagenesis PCR method using the following primers: G142A 5′-ATCTCCGGCTGGG**C**CAACACTCTGAGC-3′ and G184A 5′-ATGTTCTGTGTGG**C**CTTCCTTGAGGGA-3′. PCR products were cloned into a modified pET-17b vector (*25*). DNA sequencing was used to verify the introduction of the desired mutations.

Expression and Purification of Trypsinogen and Trypsin Mutants. Recombinant trypsinogens were expressed in *E. coli* BL21(DE3)pLysS (Novagen) as inclusion bodies and refolded *in vitro* as described previously (*26*). Zymogens were then purified by anion exchange chromatography on a Q Sepharose Fast Flow column (Amersham Biosciences) using a 0−1 M NaCl gradient in a 20 mM HEPES buffer, pH 7.0. The R193G mutant trypsinogen was loaded onto a Phenyl Sepharose Fast Flow cation exchange column (Amersham Biosciences) to prevent autoactivation. The column was equilibrated with 20 mM sodium citrate, pH 4.5, and developed with a 0−1 M NaCl gradient. Trypsinogens were

[1] Abbreviations: Fmoc, 9-fluorenylmethoxycarbonyl; HMP, 4-hydroxymethylphenoxymethyl-copolystyrene-1% divinylbenzene resin; MUGB, 4-methylumbelliferyl 4-guanidinobenzoate; SBTI, soybean trypsin inhibitor.

activated with porcine enterokinase (Sigma) at 1000:1 molar ratio in 50 mM Tris-HCl, 100 mM NaCl, 10 mM $CaCl_2$, pH 8.0. The active forms were separated by affinity chromatography on an SBTI Sepharose column (Sigma) and eluted with 10 mM HCl. Both trypsinogens and trypsins were concentrated by ultrafiltration using Vivaspin columns (Vivascience) and stored in 2.5 mM HCl in aliquots at −80 °C. Purity and homogeneity of the protein preparations were assessed by SDS-PAGE and reverse phase HPLC. Protein concentration was determined from the absorbance at 280 nm using an absorption coefficient of $\epsilon_{280} = 41\,535\ M^{-1}\ cm^{-1}$.

Differential Scanning Calorimetry. Calorimetric measurements were taken with a Microcal VP−DSC differential scanning calorimeter. Denaturation curves were recorded between 10 and 85 °C at a pressure of 2.5 atm using a scanning rate of 60 °C/h. Samples contained 0.4 mg/mL protein in 20 mM sodium phosphate, pH 8.0. Buffer scans were subtracted from the protein denaturation curves.

Circular Dichroism Spectroscopy. CD measurements were performed at 20 °C on a Jasco J 720 spectropolarimeter (JapanSpectroscopic Co.). Samples contained 0.4 mg/mL (near UV spectra) or 0.04 mg/mL (far UV spectra) protein in 20 mM sodium phosphate, pH 8.0. Spectra were recorded between 195 and 250 nm and 240−310 nm in 0.1 nm steps. Depending on the wavelength range and the protein concentration, cells with 0.1 and 1.0 cm path lengths were used. Spectra were the average of three scans.

Limited Proteolysis by Chymotrypsin. Protein samples (50 μM) were incubated in a 100 mM Tricine buffer, pH 8.0, containing 10 mM $CaCl_2$ at room temperature in the presence of bovine α-chymotrypsin (Worthington Biochemical Corporation) at a 10:1 molar ratio. At timed intervals, 6 μL aliquots were withdrawn, mixed with 2 × SDS sample buffer, and heated at 95 °C for 5 min to terminate the reaction. Proteolysis was analyzed by running the samples on 15% SDS-polyacrylamide gels under reducing conditions. Gels were stained with Brilliant Blue G for 1 h and destained with 5% methanol, 7% acetic acid overnight. The intensity of the bands was determined by densitometry using the GeneTools (Syngene) image analysis software. The linearity of the signal was assessed in the range 0.15−7.5 μg of the protein samples. In the case of active trypsin forms control experiments were carried out in the absence of chymotrypsin to take autolytic degradation into account. Experiments were also performed in the presence of 1 mM D-MePhe-Pro-Arg-aldehyde, which inhibited trypsin forms to >95% but had no affect on the activity of chymotrypsin as assessed by using chromogenic substrates. The chymotryptic cleavage site was determined by N-terminal amino acid sequencing. Proteolytic fragments were separated by SDS-PAGE, electroblotted onto a ProBlot polyvinylidene difluoride membrane (PE Biosystems) and subjected to N-terminal amino acid sequencing on a Procise 494 sequencer (Applied Biosystems).

Chemical Modification of the N-Terminus. The susceptibility of the N-terminus to chemical modification was determined by carbamylation of Ile16 with NaNCO and subsequent N-terminal sequencing by Edman degradation as described by Camire (*12*). Briefly, reaction mixtures contained 10 μM protein in 30 mM ammonium bicarbonate buffer, pH 8.0, 10 mM $CaCl_2$. The reaction was started by the addition of 0.5 M NaNCO (Aldrich), pH 8.0, and the reaction mixture was incubated at room temperature. At selected time intervals, aliquots were taken and quenched with an equal volume of 5 M hydroxylamine (Aldrich), pH 8.0. Protein samples (100 pmol) were spotted onto a ProBlot polyvinylidene difluoride membrane (PE Biosystems), and salts were removed by washing twice with 200 μL of 10% acetonitrile. N-Terminal sequence analysis was performed using a Procise 494 sequencer (Applied Biosystems), and the peak height of Ile16 was determined. Values reported are the average of three experiments. Control experiments were carried out in the presence of 0.5 M NaCl. Experiments were also performed in the presence of 1 mM D-MePhe-Pro-Arg-aldehyde. A peptide-resin corresponding to the N-terminus of human trypsin 4 was used as an unobstructed N-terminus for comparison. The IVGGYT hexapeptide was synthesized utilizing the Fmoc chemistry and using an ABI 431A (Applied Biosystems) solid-phase synthesizer. The Fmoc group was cleaved from the N-terminal Ile, while the C-terminal Thr remained attached to the HMP resin.

Proflavin Binding. The proportion of trypsin present in the active conformation was determined by mixing with proflavin in a BioLogic SFM300 stopped-flow apparatus as described by Fersht and Requena (*27*, *28*). Experiments were performed by rapidly mixing (0.25 ms dead time) equal volumes (50 μL each) of trypsin and proflavin (Sigma) to give final concentrations of 40 μM and 100 μM, respectively, in 20 mM Tricine, pH 8.0, at 20 °C. Formation of the trypsin−proflavin complex was followed spectrophotometrically at 465 nm. Several shots were averaged per experiment. No change in the absorbance signal was observed in control experiments carried out with bovine trypsinogen (Sigma).

Assay of Enzymatic Activity. Z-Gly-Pro-Arg *p*-nitroanilide (Sigma) substrate stock solutions were prepared in dimethylformamide. The final concentration of dimethylformamide in the assays was less than 1%, except in the case of G193A/G142A trypsin in which the maximal concentration was 5%. Assays were performed in 1.0 mL of assay mix containing 10 mM $CaCl_2$ in 20 mM Tricine buffer, pH 8.0, at 20 °C. The reaction was started by adding 1.22−530 nM enzyme to the reaction mixture. The hydrolysis of the substrate was monitored spectrophotometrically at 405 nm using a Shimadzu UV-2101 PC spectrophotometer. The steady-state kinetic parameters were determined from six to eight substrate concentrations between 6.25 μM and 7.5 mM as appropriate for the particular mutant trypsin. Data were analyzed by fitting to the Michaelis−Menten hyperbola using OriginPro 7.5 software, and the reported values are the average of three experiments.

Transient Kinetics. Pre-steady-state measurements were performed as described by Tóth et al. (*23*). Briefly, experiments were carried out on a KinTec SF-2004 stopped-flow apparatus equipped with a Hg-Xe superquiet lamp (Hamamatsu). Fluorescence was excited at 365 nm and monitored above 420 nm with a cutoff filter (WG420, Comar Instruments). Substrate saturation experiments were conducted using 1 μM trypsin at 4-methylumbelliferyl 4-guanidinobenzoate (MUGB, Sigma) substrate concentrations ranging from 1.95 to 500 μM in 20 mM Tricine, 10 mM $CaCl_2$, pH 8.0 at 20 °C. Several shots were averaged per experiment. Our results were also validated by using the kinetics simulation software Gepasi (*29*).

RESULTS

Expression, Purification, and Characterization of Recombinant Proteins. We substituted alanines for hinge glycines in the activation domain to assess the role of these hinges in the zymogen/active enzyme interconversion and catalytic activity of trypsin. One hinge position, i.e., Gly216, was not investigated because it also plays a direct role in catalysis by taking part in formation of the substrate binding pocket. Craik et al. introduced this mutation into rat trypsin and found that it altered the specificity of the enzyme (*30*). Alanine was chosen for substitution because our key objective was to specifically restrict conformational freedom around hinges while keeping structural perturbation to a minimum by introduction of a single methyl side chain. On the basis of structures automatically generated by SWISS-MODEL, we verified that the substitution was sterically reasonable for each mutant (*31*). Human trypsinogen 4 (193R) and its mutant forms R193G, R193A, R193G/G19A, R193G/G142A, and R193G/G184A[2] were expressed in the BL21-(DE3)pLysS strain of *E. coli* as inclusion bodies and refolded *in vitro*. Mutant trypsins were obtained by activating the appropriate trypsinogen with enterokinase and purified by affinity chromatography on SBTI resin. Stability and correct fold of the mutant proteins were verified by comparison to wild-type human trypsinogen 4 by differential scanning calorimetry and CD spectroscopy (for details see Supporting Information).

Limited Proteolysis. The global conformation of the activation domain of human trypsin 4 variants was initially probed by limited proteolysis. Limited proteolysis may be used as a structural probe to identify locally unfolded segments of a protein as cleavage sites show a good correlation with uncertain electron density and larger crystallographic temperature factors (*32*). Chain segments forming the activation domain in trypsinogen show no significant continuous electron density and are characterized by a *B*-factor of more than about 200 Å^2 (Figure 2A) (*7*, *33*). Molecular dynamics simulations also confirm that the activation domain of the zymogen exhibits increased mobility compared to the rest of the molecule (*14*).

Part of the activation domain is the autolysis loop (Gly142-Pro152), which is a conserved autolysis site in most trypsins. In contrast, the autolysis loop of human trypsin 4 does not contain a lysine; however, it contains a phenylalanine, so we hypothesized that it may be cleaved by chymotrypsin. Thus, wild-type and mutant trypsinogens and trypsins were subjected to limited proteolysis by chymotrypsin. The results of the SDS-PAGE analysis indicate that both zymogens and some active forms are cleaved very selectively at only one peptide bond, giving rise to two fragments, which are relatively resistant to further degradation. We confirmed by N-terminal amino acid sequencing that the chymotryptic cleavage occurs at peptide bond Phe147-Gly148. The time course of limited proteolysis was analyzed by first-order exponential curve fitting to densitometric data (Figure 2B,C). All the zymogen forms were found to be susceptible to limited chymotryptic proteolysis (Table 1). Moreover, a similar cleavage efficiency was observed in all cases (k_{obs} = 0.052−0.17 min^{-1}). By contrast, the activated enzymes revealed completely different behavior (Table 1). Wild-type human trypsin 4 as well as the R193G and the R193G/G19A mutants were completely resistant to chymotryptic degradation. The R193A mutant revealed low susceptibility to limited proteolysis (k_{obs} = 0.003 min^{-1}). Yet, the R193G/G142A and the R193G/G184A mutants were characterized by an increased susceptibility to chymotryptic cleavage with ob-

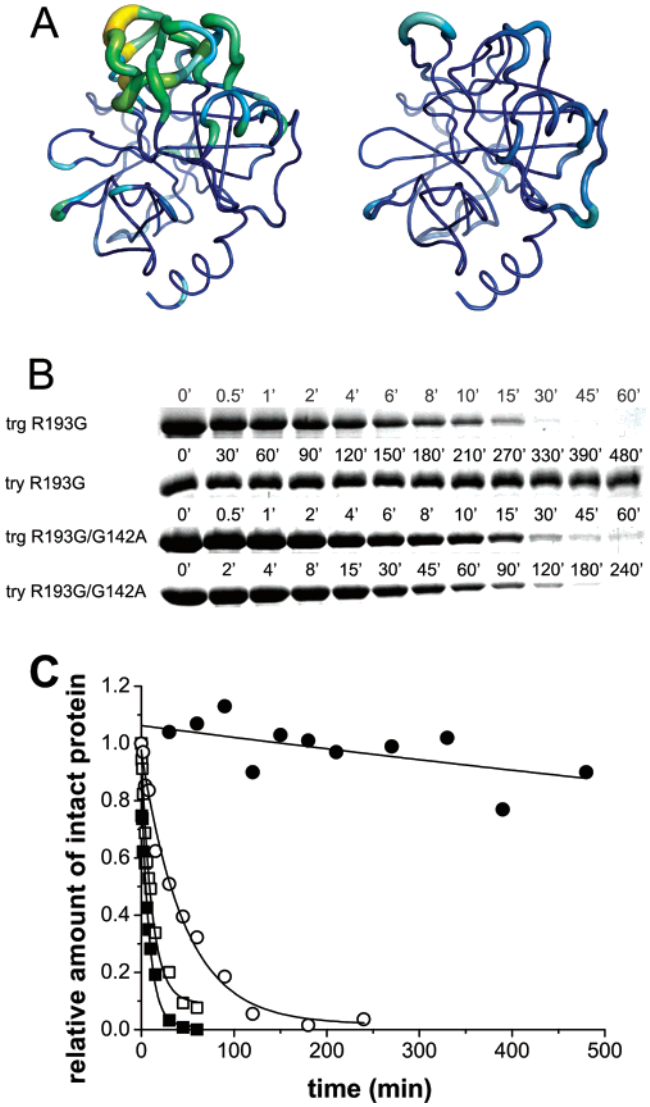

FIGURE 2: Limited proteolysis of zymogens and active forms of human trypsin 4 variants by chymotrypsin. (A) The *B*-factor distribution of bovine trypsinogen (left) and trypsin (right). Colors are scaled so that dark blue indicates low *B*-factors, while residues with high *B*-factors are shown in yellow. Residues composing the activation domain of trypsinogen show significantly higher *B*-factors than the rest of the molecule. By contrast, the active form contains considerably less residues with high *B*-factors evenly distributed on the surface of the molecule. The figure was prepared using the structures 1TGN and 2BLV and the program PyMOL (DeLano Scientific) (*21*). Human trypsin 4 variants were subjected to limited proteolysis by bovine α chymotrypsin at a 10:1 molar ratio in 100 mM Tricine, pH 8.0, containing 10 mM $CaCl_2$ at room temperature. Proteolysis was monitored by SDS-PAGE followed by densitometry. (B) Brilliant Blue G stained gels of digestion reactions. (C) The time course of limited chymotryptic proteolysis of the R193G zymogen (■) and activated (●) and the R193G/G142A zymogen (□) and activated (○) human trypsin 4 variants.

[2] Human trypsin 4 carries an arginine at position 193 so the R193G variant is a mutant. On the other hand, the evolutionary ancient and widespread residue at this position is glycine in serine proteases so the R193G mutant is taken as a reference form for comparison of our results.

Table 1: Observed Rate Constants of Chymotryptic Digestion of the Zymogen and the Active Form of Selected Variants of Human Trypsin 4

	k_{obs} (min^{-1})	
	zymogen	active enzyme
wt (193R)	0.16 ± 0.01	<0.001
R193G	0.12 ± 0.02	<0.001
R193A	0.17 ± 0.01	0.0017 ± 0.0003
R193G/G19A	0.14 ± 0.01	<0.001
R193G/G142A	0.087 ± 0.006	0.022 ± 0.002
R193G/G184A	0.052 ± 0.005	0.011 ± 0.002

served rate constants of 0.022 and 0.011 min^{-1}, respectively. These results indicate that the activation domain of the mutant trypsins may be disordered similarly to that of the zymogen form. This supports the idea that restriction of the conformational flexibility around hinges of the activation domain may result in a zymogen-like conformation of the active enzyme. In the case of the completely resistant R193G variant and the R193G/G142A mutant, which is the most susceptible form to chymotryptic degradation, limited proteolytic experiments were also carried out in the presence of the tetrahedral intermediate analogue D-MePhe-Pro-Arg-aldehyde (*34*). The disparity in the susceptibility to chymotryptic proteolysis disappeared in the presence of the inhibitor as the R193G/G142A mutant became resistant to proteolytic degradation ($k_{obsR193G} < 0.001$ min^{-1}, $k_{obsR193G/G142A} = 0.0018 \pm 0.0006$ min^{-1}).

Chemical Modification of the N-Terminus. A zymogen-like conformation is characterized by destabilized salt bridge formation between Ile16 and Asp194. If the N-terminus is not stably inserted into the activation pocket, it should be more readily available for chemical modification of the N-terminal primary amine. In order to test this idea, trypsin variants were reacted with NaNCO, which preferentially modifies the N-terminus on proteins (*35*, *36*), and the rate of disappearance of the Ile16 signal was monitored by N-terminal sequence analysis. A faster rate of carbamylation indicates impaired and destabilized salt bridge formation. As shown in Figure 3A, wild-type human trypsin 4 as well as the R193G and the R193A mutants are characterized by a relatively low susceptibility of the N-terminus to be chemically modified with 75%, 59%, and 58% unmodified N-terminus after 4 h, respectively. In contrast, the rate of carbamylation of the double-mutants is faster: only 36% of the R193G/G184A mutant, 20% of the R193G/G19A mutant, and 12% of the R193G/G142A mutant was found to be unmodified after 4 h (Figure 3A). This indicates that the N-terminus of these three mutants is significantly more exposed, suggesting a zymogen-like conformation of the active enzyme. The IVGGYT peptide-resin corresponding to the first six amino acids of human trypsin 4 was used as a control representing an unobstructed N-terminus. The rate of carbamylation of the R193G/G19A and the R193G/G142A mutants was comparable with that of the free N-terminus with 14% remaining unmodified after 4 h. Again, the disparity in the susceptibility of the N-terminus to chemical modification disappeared in the presence of the substrate analogue D-MePhe-Pro-Arg-aldehyde (Figure 3B). While the presence of the inhibitor did not influence the accessibility of the N-terminus of the R193G reference form (66% remained unmodified after 4 h), the exposure of the N-terminus of the R193G/G19A mutant significantly decreased compared to the free enzyme: 56% was found to be unmodified after 4 h.

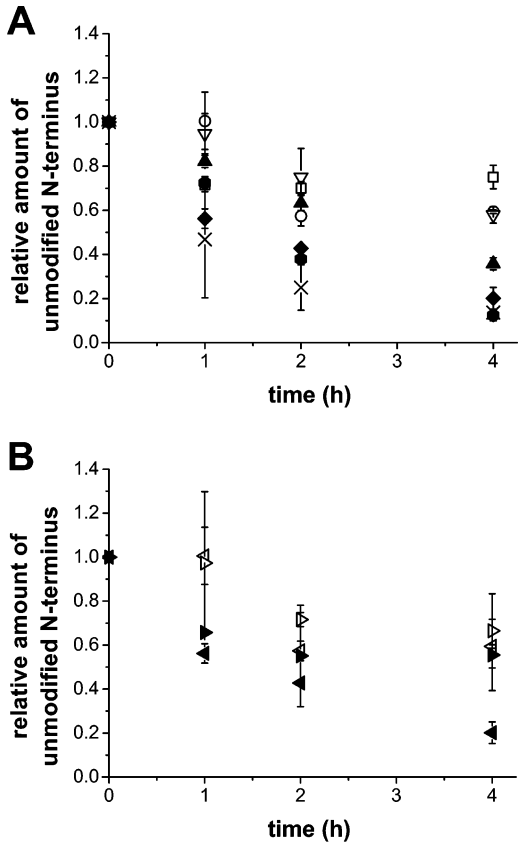

FIGURE 3: Chemical modification of the N-terminus of human trypsin 4 variants by NaNCO. Reaction mixtures containing 10 μM trypsin in 30 mM ammonium bicarbonate, 10 mM $CaCl_2$, pH 8.0, were reacted with 0.5 M NaNCO at room temperature. At selected time intervals an aliquot of the reaction mixture was mixed with 5 M hydroxylamine, pH 8.0 and subjected to N-terminal sequence analysis. Experiments were also performed in the presence of 1 mM D-MePhe-Pro-Arg-aldehyde. (A) The relative amount of sequencable N-terminus of wild-type human trypsin 4 (□) ant its mutants R193G (○), R193A (▽), R193G/G19A (◆), R193G/G142A (●), R193G/G184A (▲) and the IVGGYT peptide-resin (×) as a control corresponding to an unobstructed N-terminus is plotted at quenching times of 0, 1, 2, and 4 h. (B) The effect of active site occupation by the substrate analogue D-MePhe-Pro-Arg-aldehyde on the rate of carbamylation: the relative amount of free N-terminus of the R193G free (left-pointing open triangle) and inhibited (right-pointiing open triangle) and the R193G/G142A free (left-pointing solid triangle) and inhibited (right-pointing solid triangle) mutants.

Proflavin Binding. The results of limited proteolytic and chemical modification experiments indicate a zymogen-like conformation of the active form of the mutant enzymes. The exact proportion of the active conformation and the inactive, zymogen-like conformation was determined by proflavin binding. The fraction of active conformation at pH 8.0 was determined by following the formation of the trypsin−proflavin complex by stopped-flow spectrophotometry (*27*, *28*). Proflavin is an acridine dye which combines reversibly with the active site of trypsin and other serine proteases, resulting in large absorption spectrum changes (*37*, *38*). Proflavin may be used as a direct probe of the integrity of the active site. Namely, it binds specifically to the S1 binding pocket of the active conformation while it does not bind to the zymogen form, where the S1 binding pocket is collapsed.

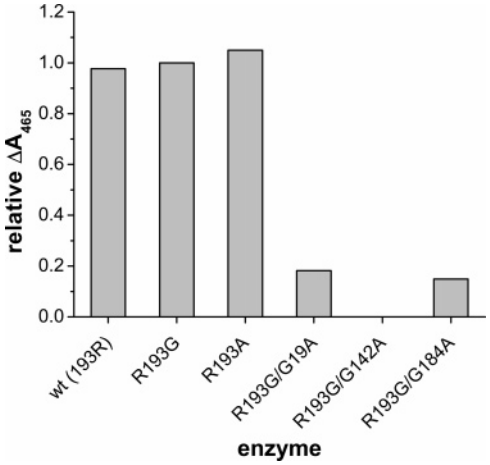

FIGURE 4: Proflavin binding by wild-type human trypsin 4 and its mutant forms. The increase in absorbance at 465 nm upon mixing human trypsin 4 variants with excess proflavin relative to the R193G mutant. A 40 μM concentration of each enzyme variant was mixed with 100 μM proflavin in 20 mM Tricine pH 8.0 at 20 °C.

Upon rapidly mixing human trypsin 4 variants with excess proflavin, a burst with a rate constant $\geq$1000 s^{-1} was observed. The amplitude of the burst for each mutant was compared to the value observed for the R193G mutant (Figure 4) as we assumed that, similarly to other trypsins carrying glycines in all hinges, over 99% of this variant must be in the active conformation (*13*, *39*). The wild-type and the R193A forms displayed bursts with similar amplitudes (98% and 105% of the R193G reference form, respectively) as the R193G mutant, indicating that all variants at position 193 are present in the active conformation. By contrast, a significant decrease in the amplitude was observed for all other mutants. The R193G/G19A and the R193G/G184A mutants revealed bursts with significantly smaller amplitudes, i.e., 18 and 15% of the R193G form, respectively. The largest effect was observed for the R193G/G142A substitution, as this mutant gave no burst upon mixing with proflavin. These data demonstrate that the active site is not properly formed in the mutant enzymes.

Kinetic Measurements. We initially studied the effects of restriction in the conformational flexibility around activation domain hinges in trypsin catalysis by measuring catalytic activity using a good chromogenic amide substrate. Table 2 summarizes the steady-state kinetic data for the hydrolysis of Z-Gly-Pro-Arg *p*-nitroanilide by wild-type and mutant forms of human trypsin 4. Comparison of Gly193 with residues carrying a side chain, e.g., alanine or arginine results in only a slight change in the catalytic efficiency (1.2- and 1.1-fold increase, respectively), as the R193A mutant and wild-type human trypsin 4 revealed an ~1.5-fold increase both in K_M and k_{cat}, when compared to the R193G mutant. The three other mutant forms revealed different kinetic properties. They were all characterized by a reduced catalytic efficiency mainly as a result of an increase in K_M. The R193G/G19A mutant gave a close to normal k_{cat} value; however, it revealed a 4.1-fold reduced catalytic efficiency, mainly because of an increase in K_M. A 17-fold increase in the K_M value along with a 1.9-fold decrease in k_{cat} was observed for the R193G/G184A mutant form, leading to a 32-fold lower catalytic efficiency. The most dramatic change was observed for the R193G/G142A mutant with an ~700-fold increase in the K_M value together with a 14-fold decrease in k_{cat}. Together, it led to a 10^4-fold decrease in the catalytic efficiency as compared with the R193G single-mutant.

To obtain further insight into the mechanisms of the catalytic activity of the mutant trypsins, pre-steady-state kinetics of the enzyme reactions were also analyzed. We chose 4-methylumbelliferyl 4-guanidinobenzoate (MUGB) fluorogenic substrate analogue in an experimental setup that permits the separation of elementary reaction steps of substrate hydrolysis and the determination of their rate constants (*23*). For wild-type human trypsin 4 and the R193G mutant, Tóth et al. found that the time course of fluorescence change under pseudo-first-order conditions showed a burst phase followed by a linear phase. The burst could be described by two exponentials: the fast phase is due to the formation of the first tetrahedral intermediate while the slow phase corresponds to the formation of the covalent acyl-enzyme. The linear phase is the result of slow deacylation. On the basis of structural and steady-state kinetic data we assumed that the introduced mutations do not cause drastic changes in the reaction mechanism. However, the equilibrium between the inactive, zymogen-like and the active, trypsin-like conformations has to be considered (Scheme 1).

Similarly to the case of wild-type human trypsin 4 and its R193G mutant, the time course of MUGB hydrolysis by all selected trypsin variants was well described by a burst phase followed by a linear phase (Figure 5). For the R193A, the R193G/G19A and the R193G/G184A mutant forms the burst consisted of two exponentials, whereas in the case of the R193G/G142A mutant the burst phase could be described by a single-exponential function (for details of the data analysis see Supporting Information). The observed rate constants are shown in Table 3. For the R193A variant the observed rate constants for both phases ($k_{obsfast}$ = 17 s^{-1} and $k_{obsslow}$ = 0.28 s^{-1}) were comparable with those for the R193G mutant and the wild-type enzyme indicating essentially the same reaction mechanism for the R193A mutant as reported previously for the other two variants at position 193. In contrast, the other three mutant forms revealed different kinetic properties that could not be explained solely on the grounds of the model proposed for the variants at position 193. While the observed rate constant of the fast phase for the R193G/G19A mutant was only slightly smaller ($k_{obsfast}$ = 15 s^{-1}) than for the R193G form, it decreased 41-fold for the R193G/G184A mutant ($k_{obsfast}$ = 0.59 s^{-1}). The observed rate constants of the slow phase of these two mutants and that of the burst of the R193G/G142A mutant were all comparable ($k_{obsslow}$ = 4.7 $\times$ 10^{-2} s^{-1} for R193G/G19A, k_{obs} = 6.9 $\times$ 10^{-2} s^{-1} for R193G/G142A, and $k_{obsslow}$ = 5.1 $\times$ 10^{-2} s^{-1} for R193G/G184A) but much smaller than for the variants at position 193. Moreover, the slow phase for the R193G/G19A and the R193G/G184A mutants became independent of the substrate concentration above extremely low half-saturation concentrations (1.1 and 4 μM, respectively), indicating a process occurring prior to substrate binding.

The fluorescent signal is generated during formation of the first tetrahedral intermediate resulting in the appearance of the fast phase (*23*). For the zymogen-like mutants only the enzyme fraction in the active conformation may enter the catalytic cycle and form the tetrahedral intermediate; therefore, the fast phase corresponds to the active trypsin-

Table 2: Steady-State Kinetic Parameters of Wild-Type Human Trypsin 4 and Its Mutant Forms[a]

	k_{cat} (s^{-1})	K_M (μM)	k_{cat}/K_M (M^{-1} s^{-1})	relative k_{cat}/K_M[b]
wt (193R)	88.2 ± 2.5	29.8 ± 3.1	$(2.96 \pm 0.32) \times 10^6$	1.1
R193G	54.1 ± 1.2	20.3 ± 1.6	$(2.67 \pm 0.22) \times 10^6$	1
R193A	83.6 ± 2.0	26.6 ± 2.4	$(3.14 \pm 0.29) \times 10^6$	1.2
R193G/G19A	51.5 ± 0.5	78.8 ± 2.1	$(6.54 \pm 0.19) \times 10^5$	0.25
R193G/G142A	≥3.86 ± 0.76	≥ $(14.1 \pm 3.98) \times 10^3$	$(2.74 \pm 0.94) \times 10^2$	1.0×10^{-4}
R193G/G184A	29.2 ± 0.4	346 ± 13	$(8.44 \pm 0.34) \times 10^4$	3.2×10^{-2}

[a] Increasing amounts of the substrate Z-Gly-Pro-Arg *p*-nitroanilide were added to reactions containing 1.22−530 nM enzyme in 20 mM Tricine, 10 mM $CaCl_2$, pH 8.0 at 20 °C. [b] The relative k_{cat}/K_M is calculated from the ratio of the k_{cat}/K_M of each trypsin form to that of the R193G mutant.

Scheme 1: Expanded Mechanism for MUGB Hydrolysis[a]

$$Z \rightleftharpoons E + MUGB \underset{k_{-1}}{\overset{k_1}{\rightleftharpoons}} E{\bullet}MUGB \underset{k_{-2}}{\overset{k_2}{\rightleftharpoons}} E\text{-}GB\text{-}MU^* \xrightarrow{k_3} E\text{-}GB + MU^* \xrightarrow{k_4} E + GB$$

[a] MUGB hydrolysis includes substrate binding (step 1), formation of the first tetrahedral intermediate (step 2), formation of the covalent acyl-enzyme (step 3), and slow deacylation (step 4). This reaction mechanism is expanded by the conformational equilibrium between an inactive, zymogen-like and an active form. Z, zymogen-like conformation; E, active conformation; MUGB, 4-methylumbelliferyl 4-guanidinobenzoate; GB, 4-guanidinobenzoate; MU, 4-methylumbelliferone; fluorescent species are denoted with an asterisk.

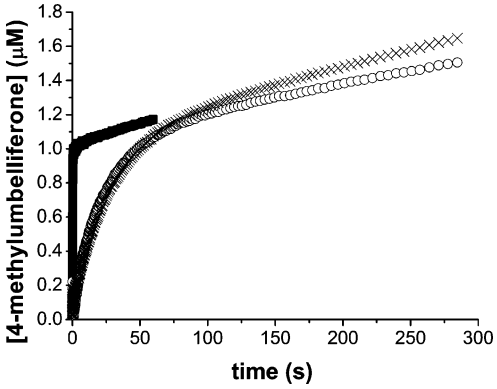

FIGURE 5: Time course of the reaction of human trypsin 4 mutants R193A (■), R193G/G19A (×), and R193G/G142A (○) with 4-methylumbelliferyl 4-guanidinobenzoate (MUGB) substrate analogue. A 1 μM concentration of enzyme was mixed with 500 μM MUGB in 20 mM Tricine, 10 mM $CaCl_2$, pH 8.0, at 20 °C. Fluorescence of the product 4-methylumbelliferone was excited at 365 nm and monitored above 420 nm.

Table 3: Kinetic Parameters of Human Trypsin 4 Variants on MUGB Substrate Analogue[a]

	$k_{obsfast}$ (s^{-1})	$k_{obsslow}$ (s^{-1})	k_4 (s^{-1})
wt (193R)[b]	10	0.42	1.9×10^{-3}
R193G[b]	24	1.4	3.3×10^{-4}
R193A	17	0.28	1.3×10^{-3}
R193G/G19A	15	4.7×10^{-2}	1.6×10^{-3}
R193G/G142A	n.d.	6.9×10^{-2}	2.7×10^{-3}
R193G/G184A	0.59	5.1×10^{-2}	2.0×10^{-3}

[a] Observed rate constants of the two exponential phases of the burst and the rate constant of deacylation. Fluorescence stopped-flow experiments were performed using 1 μM trypsin and MUGB concentrations ranging from 1.95 to 500 μM depending on the enzyme variant in 20 mM Tricine, 10 mM $CaCl_2$, pH 8.0 at 20 °C. Fluorescence of the product 4-methylumbelliferone was excited at 365 nm and monitored above 420 nm. Apparent rate constants were determined by fitting second-order exponentials followed by a linear phase to the transients. The rate constant of deacylation was calculated according to Tóth et al. (*23*). [b] Data from Tóth et al. rounded to two digits (*23*)

like fraction. In the case of the R193G/G142A mutant, whose active site is completely in an inactive conformation according to the results of proflavin binding, no fast phase could be observed, also indicating that the active fraction is negligible. The simplest model that explains the origin of the slow phase for the zymogen-like mutants, in accordance with the results of the structural probes and steady-state kinetics, is that the slow phase emerges from the inactive to active transition. Substrate binding by the enzyme fraction in the active conformation decreases the concentration of the free active enzyme, shifting the inactive/active equilibrium toward the active form. As the inactive to active transition is very slow it will represent the rate-limiting step, and acylation cannot be resolved.

DISCUSSION

We have investigated the role of glycine hinges of the activation domain in the zymogen/active interconversion and catalytic activity of trypsin. These glycine residues are highly conserved in serine proteases, indicating a crucial role in the overall protein architecture. The importance of the hinge glycines for enzymatic function is underscored by the fact that the substitution of any of these glycines in serine protease factors involved in blood coagulation, e.g., factors VII, IX and X, leads to bleeding disorders (*40*−*43*). Only phenotypical data have been available on these mutations; however, our work sheds light on the molecular mechanism of these hemophilias. On the basis of a molecular dynamics simulation, Brünger et al. suggested that substitution or removal of the key residues involved in trypsinogen activation will presumably induce larger scale changes in the protein structure (*14*). The contribution of the salt bridge between Ile16 and Asp194 as well as hydrophobic interactions of the Ile16 side chain to the activation process has been extensively studied (*39*, *44*). On the other hand, the structural and functional role of glycine hinges of the activation domain has not been studied so far.

We replaced hinge glycines by alanines to keep structural perturbation at a minimum. Indeed, none of the mutations studied here caused any significant change in the ordered secondary and tertiary structure of the zymogens as assessed by their CD spectra and thermal stability. In contrast, the mutations affected the structure of the activation domain in the activated enzymes. We probed all the features distinctive for the zymogen form, i.e., increased flexibility of the autolysis loop, a free N-terminus and a deformed active site and found that the mutant forms show zymogen-like structures. However, the extent of these changes was widely different (Table 4). Position 193 proved to be the least sensitive to perturbation: wild-type human trypsin 4 containing an arginine at position 193 and the R193A mutants showed active structures similar to the R193G reference form. This is consistent with the fact that naturally occurring isoforms are only reported for position 193 among the hinge positions studied here (*45*, *46*). The other three hinge

Table 4: Percentage of the Active Conformation in the Activated Form of Human Trypsin 4 Variants According to Different Experimental Approaches

	ordered autolysis loop (limited proteolysis, Figure 2)[a]	buried N-terminus (chemical modification, Figure 3)[b]	correctly formed active site proflavin binding, Figure 4)	catalytic activity (Table 2)
wt (193R)	100	88	100	100
R193G	100	83	100	100
R193A	90	85	100	100
R193G/G19A	100	51	18	25
R193G/G142A	75	50	<1	<1
R193G/G184A	79	73	15	3

[a] Calculated by dividing the observed rate constant of the activated form by that of the corresponding zymogen. [b] Calculated by dividing the observed rate constant of the activated form by that of the control peptide IVGGYT corresponding to an unobstructed N-terminus. Observed rate constants were calculated by first-order exponential curve fitting.

positions were found to be more sensitive to perturbation of the conformational flexibility, although to variable extents. The R193G/G184A mutant revealed only a partially zymogen-like, while the R193G/G142A variant a more typical zymogen-like structure. The data for the R193G/G142A mutant may be explained by the additional role of Gly142 in the stabilization of the active conformation by hydrogen bonding interactions to both the N-terminal Ile16 and Asp194. Thus, this position may be particularly sensitive to perturbation. The R193G/G19A mutant may also be regarded as a kind of zymogen-like trypsin on the basis of its relatively more exposed N-terminus and deformed active site. These zymogen-like properties, however, are not consistent with the resistance of its autolysis loop to limited proteolysis. In this context it is interesting to note that in human trypsin 4 there is a direct contact of the N-terminus to the substrate binding site: there are two hydrogen bonds connecting Val17N to Asp189O and Asp189N to Val17O. A conformational change of the N-terminus may thus be directly transferred to the active site without significantly affecting the structure of other activation domain segments.

Variations in the results of the different conformational probes suggest that the hinge mutants represent different structural intermediates between the inactive trypsinogen-like and active trypsin conformations. These results are consistent with low-temperature crystallography data showing that the activation domain of trypsinogen itself exists in a number of closely related but different conformations (*33*). Furthermore, perturbed angular γ-correlation spectroscopy showed that there is interconversion among these conformers on the nanosecond time scale, while no dynamics occur in this time range in the trypsin-like state (*47*).

Binding of the tetrahedral intermediate analogue D-MePhe-Pro-Arg-aldehyde to mutants with a zymogen-like conformation restores the active structure. These results confirm that the conformation of the trypsin molecule does not undergo substantial structural deformation due to the introduced mutations. Instead, the equilibrium between the well-defined trypsin-like conformation and zymogen-like conformations may be pushed to the zymogen-like states. Binding of the substrate analogue may shift the equilibrium toward the active form by stabilizing the trypsin-like conformation.

Applying the Michaelis−Menten model to the hydrolysis of the amide substrate Z-Gly-Pro-Arg *p*-nitroanilide by our set of trypsin mutants, the catalytic efficiency shows a pronounced tendency to decrease correlating with the zymogenity of the structure. Similarly, analysis of Ile16 mutant trypsins revealed that stability of the activation domain correlates with k_{cat}/K_M (*39*). Comparing the results of the kinetic measurements and the structural probes, our data show that the catalytic efficiency correlates with the conformation of the active site, while it is rather independent of the structural state of the N-terminus and the autolysis loop (Table 4). This implies that the enzyme activity requires a fixed conformation of the S1 site (like that of mutant R193G/19A), which, on the other hand, can be supported by varying conformations of the N-terminus and the autolysis loop. In accordance with the recent results, the crystal structures of trypsinogen mutants with increased activity in complex with bovine pancreatic trypsin inhibitor revealed an S1 site and oxyanion hole conformation similar to trypsin but different conformations of the N-terminal segment and the autolysis loop (*48*). The reduction of the catalytic efficiency is mainly due to an increase of K_M, while the value of k_{cat} is only moderately affected by the mutations. A 14-fold reduction of k_{cat} may only be observed for the R193G/G142A mutant but this value could not be well determined because of the high K_M of this mutant. These results indicate that the mutations do not perturb the catalytic machinery to a great extent. One explanation for the elevated K_M value might be a defective substrate binding. However, the increase of K_M parallel to the results of the structural probes suggests that the inactive/active equilibrium is shifted toward the inactive form, and high substrate concentration is needed to push the equilibrium toward the active conformation. Transient kinetic measurements of MUGB hydrolysis, which permit the separation of individual reaction steps, confirmed the existence of the inactive to active conformational transition prior to substrate binding. Still, the mutations may also exert an effect on the formation of the first tetrahedral intermediate, and a decrease of the rate constant correlates with the zymogenity of the structure. As subsequent steps, e.g., acylation and deacylation, are much less affected by the introduced mutations, we propose that the enzyme structure is restored during the formation of the first tetrahedral intermediate by an induced fit mechanism. These findings are consistent with the results of limited proteolysis and N-terminal modification in the presence of tetrahedral intermediate analogues and the relatively unaffected k_{cat} values of the steady-state measurements. Our results are also supported by thermodynamic and isotope effect studies which revealed that extended substrates are able to induce a conformational isomerization of the enzyme coupled to active site chemistry during formation of the acyl-enzyme that promotes catalysis (*49*, *50*). In accordance with our data Hedstrom et al. found that mutations of the Ile16 side chain,

which destabilize the activation domain of trypsin, selectively decrease the rate of acylation, while substrate binding and deacylation are not effected (*39*).

In summary, replacement of hinge glycines by alanines perturbs formation of the active conformation to various extents. All variants at position 193 are fully active. Mutations at all other positions shift the inactive/active equilibrium toward the inactive zymogen-like state. This phenomenon fully explains the structural and kinetics properties of the mutant R193G/G19A. Replacements of the hinge glycines at positions 184 and 142, however, cause more extended structural perturbations. Our data show that in the absence of substrate, the mutant R193G/G184A does not exist in a fully active structural form. Conformational transition to result in a fully active structure of this mutant may only occur in the course of catalysis when the tetrahedral intermediate is formed. Thus, this can be due to a mechanism of induced fit. In the case of the replacement at position 142 the active structure cannot be fully restored. We believe that our hinge mutants with all these various properties will serve as good models to further explore the role of structural plasticity in the mechanism of serine protease action and in protein function in general.

ACKNOWLEDGMENT

We thank Emi Énekes for expert technical assistance in the preparation of recombinant enzymes. We also thank Dr. Sándor Bajusz for the gift of the tripeptide aldehyde. We are grateful to Dr. Mihály Kovács for valuable discussions.

SUPPORTING INFORMATION AVAILABLE

Detailed description of the results of differential scanning calorimetry and CD-spectroscopy along with far-UV and near-UV CD spectra of human trypsin 4 variants (Figure S1) and detailed analysis of MUGB hydrolysis: time course of the reaction fitted to both single and double exponential functions with a steady-state term (Figure S2) and dependence of the observed rate constants of the phases of the burst for human trypsin 4 mutants on MUGB concentration (Figure S3). This material is available free of charge *via* the Internet at http://pubs.acs.org.

REFERENCES

1. Barrett, A. J., Rawlings, N. D., and Woessner, F. F., Jr. (Eds). (1998) *Handbook of proteolytic enzymes*, Academic Press, San Diego, CA.
2. Hedstrom, L. (2002) Serine protease mechanism and specificity, *Chem. Rev. 102*, 4501−4524.
3. de Haën, C., Neurath, H., and Teller, D. C. (1975) The phylogeny of trypsin-related serine proteases and their zymogens. New methods for the investigation of distant evolutionary relationships, *J. Mol. Biol. 92*, 225−259.
4. Neurath, H. (1984) Evolution of proteolytic enzymes, *Science 224*, 350−357.
5. Khan, A. R., and James, M. N. (1998) Molecular mechanisms for the conversion of zymogens to active proteolytic enzymes, *Protein Sci. 7*, 815−836.
6. Bode, W., and Schwager, P. (1975) The refined crystal structure of bovine beta-trypsin at 1.8 Å resolution. II. Crystallographic refinement, calcium binding site, benzamidine binding site and active site at pH 7.0, *J. Mol. Biol. 98*, 693−717.
7. Fehlhammer, H., Bode, W., and Huber, R. (1977) Crystal structure of bovine trypsinogen at 1.8 Å resolution. II. Crystallographic refinement, refined crystal structure and comparison with bovine trypsin, *J. Mol. Biol. 111*, 415−438.
8. Bode, W., Schwager, P., and Huber, R. (1978) The transition of bovine trypsinogen to a trypsin-like state upon strong ligand binding. The refined crystal structures of the bovine trypsinogen-pancreatic trypsin inhibitor complex and of its ternary complex with Ile-Val at 1.9 Å resolution, *J. Mol. Biol. 118*, 99−112.
9. Pasternak, A., Ringe, D., and Hedstrom, L. (1999) Comparison of anionic and cationic trypsinogens: the anionic activation domain is more flexible in solution and differs in its mode of BPTI binding in the crystal structure, *Protein Sci. 8*, 253−258.
10. Fersht, A. R. (1971) Conformational equilibria and the salt bridge in chymotrypsin, *Cold Spring Harbor Symp. Quant. Biol. 36*, 71−73.
11. Spomer, W. E., and Wootton, J. F. (1971) The hydrolysis of alpha-N-benzoyl-L-argininamide catalyzed by trypsin and acetyltrypsin. Dependence on pH, *Biochim. Biophys. Acta 235*, 164−171.
12. Camire, R. M. (2002) Prothrombinase assembly and S1 site occupation restore the catalytic activity of FXa impaired by mutation at the sodium-binding site, *J. Biol. Chem. 277*, 37863−37870.
13. Huber, R., and Bode, W. (1978) Structural basis of the activation and action of trypsin, *Acc. Chem. Res. 11*, 114−122.
14. Brünger, A. T., Huber, R., and Karplus, M. (1987) Trypsinogen−trypsin transition: a molecular dynamics study of induced conformational change in the activation domain, *Biochemistry 26*, 5153−5162.
15. Wroblowski, B., Díaz, J. F., Schlitter, J., and Engelborghs, Y. (1997) Modelling pathways of alpha-chymotrypsin activation and deactivation, *Protein Eng. 10*, 1163−1174.
16. Mátrai, J., Verheyden, G., Krüger, P., and Engelborghs, Y. (2004) Simulation of the activation of alpha-chymotrypsin: analysis of the pathway and role of the propeptide, *Protein Sci. 13*, 3139−3150.
17. Kirchhofer, D., Lipari, M. T., Santell, L., Billeci, K. L., Maun, H. R., Sandoval, W. N., Moran, P., Ridgway, J., Eigenbrot, C., and Lazarus, R. A. (2007) Utilizing the activation mechanism of serine proteases to engineer hepatocyte growth factor into a Met antagonist, *Proc. Natl. Acad. Sci. U.S.A. 104*, 5306−5311.
18. Wiegand, U., Corbach, S., Minn, A., Kang, J., and Müller-Hill, B. (1993) Cloning of the cDNA encoding human brain trypsinogen and characterization of its product, *Gene 136*, 167−175.
19. Nyaruhucha, C. N., Kito, M., and Fukuoka, S. I. (1997) Identification and expression of the cDNA-encoding human mesotrypsin-(ogen), an isoform of trypsin with inhibitor resistance, *J. Biol. Chem. 272*, 10573−10578.
20. Rowen, L., Williams, E., Glusman, G., Linardopoulou, E., Friedman, C., Ahearn, M. E., Seto, J., Boysen, C., Qin, S., Wang, K., Kaur, A., Bloom, S., Hood, L., and Trask, B. J. (2005) Interchromosomal segmental duplications explain the unusual structure of PRSS3, the gene for an inhibitor-resistant trypsinogen, *Mol. Biol. Evol. 22*, 1712−1720.
21. DeLano, W. L. (2002), DeLano Scientific, Palo Alto, CA.
22. Tóth, J., Simon, Z., Medveczky, P., Gombos, L., Jelinek, B., Szilágyi, L., Gráf, L., and Málnási-Csizmadia, A. (2007) Site directed mutagenesis at position 193 of human trypsin 4 alters the rate of conformational change during activation: role of local internal viscosity in protein dynamics, *Proteins 67*, 1119−1127.
23. Tóth, J., Gombos, L., Simon, Z., Medveczky, P., Szilágyi, L., Gráf, L., and Málnási-Csizmadia, A. (2006) Thermodynamic analysis reveals structural rearrangement during the acylation step in human trypsin 4 on 4-methylumbelliferyl 4-guanidinobenzoate substrate analogue, *J. Biol. Chem. 281*, 12596−12602.
24. Gráf, L. (1995) Structural basis of serine protease action: the fourth dimension, in *Natural sciences and human thought* (Zwilling, R., Ed.) pp 139−148, Springer, Berlin, Germany.
25. Katona, G., Berglund, G. I., Hajdu, J., Gráf, L., and Szilágyi, L. (2002) Crystal structure reveals basis for the inhibitor resistance of human brain trypsin, *J. Mol. Biol. 315*, 1209−1218.
26. Szilágyi, L., Kénesi, E., Katona, G., Kaslik, G., Juhász, G., and Gráf, L. (2001) Comparative in vitro studies on native and recombinant human cationic trypsins. Cathepsin B is a possible pathological activator of trypsinogen in pancreatitis, *J. Biol. Chem. 276*, 24574−24580.
27. Fersht, A. R., and Requena, Y. (1971) Equilibrium and rate constants for the interconversion of two conformations of α-chymotrypsin. The existence of a catalytically inactive conformation at neutral pH, *J. Mol. Biol. 60*, 279−290.
28. Fersht, A. R. (1972) Conformational equilibria in α-and γ-chymotrypsin. The energetics and importance of the salt bridge, *J. Mol. Biol. 64*, 497−509.

29. Mendes, P. (1993) GEPASI: a software package for modelling the dynamics, steady states and control of biochemical and other systems, *Comput. Appl. Biosci. 9*, 563−571.
30. Craik, C. S., Largman, C., Fletcher, T., Roczniak, S., Barr, P. J., Fletterick, R., and Rutter, W. J. (1985) Redesigning trypsin: alteration of substrate specificity, *Science 228*, 291−297.
31. Schwede, T., Kopp, J., Guex, N., and Peitsch, M. C. (2003) SWISS-MODEL: An automated protein homology-modeling server, *Nucleic Acids Res. 31*, 3381−3385.
32. Hubbard, S. J. (1998) The structural aspects of limited proteolysis of native proteins, *Biochim. Biophys. Acta 1382*, 191−206.
33. Walter, J., Steigemann, W., Singh, T. P., Bartunik, H., Bode, W., and Huber, R. (1982) On the disordered activation domain in trypsinogen: chemical labelling and low-temperature chrystallography, *Acta Crystallogr., Sect. B: Struct. Crystallogr. Cryst. Chem. 38*, 1462−1472.
34. Ortiz, C., Tellier, C., Williams, H., Stolowich, N. J., and Scott, A. I. (1991) Diastereotopic covalent binding of the natural inhibitor leupeptin to trypsin: detection of two interconverting hemiacetals by solution and solid-state NMR spectroscopy, *Biochemistry 30*, 10026−10034.
35. Stark, G. R., Stein, W. H., and Moore, S. (1960) Reactions of the cyanate present in aqueous urea with amino acids and proteins, *J. Biol. Chem. 235*, 3177−3181.
36. Plapp, B. V., Moore, S., and Stein, W. H. (1971) Activity of bovine pancreatic deoxyribonuclease A with modified amino groups, *J. Biol. Chem. 246*, 939−945.
37. Bernhard, S. A., and Gutfreund, H. (1965) The optical detection of transients in trypsin- and chymotrypsin-catalyzed reactions, *Proc. Natl. Acad. Sci. U.S.A. 53*, 1238−1243.
38. Conti, E., Rivetti, C., Wonacott, A., and Brick, P. (1998) X-ray and spectrophotometric studies of the binding of proflavin to the S1 specificity pocket of human alpha-thrombin, *FEBS Lett. 425*, 229−233.
39. Hedstrom, L., Lin, T. Y., and Fast, W. (1996) Hydrophobic interactions control zymogen activation in the trypsin family of serine proteases, *Biochemistry 35*, 4515−4523.
40. Bernardi, F., Castaman, G., Pinotti, M., Ferraresi, P., Di Iasio, M. G., Lunghi, B., Rodeghiero, F., and Marchetti, G. (1996) Mutation pattern in clinically asymptomatic coagulation factor VII deficiency, *Hum. Mutat. 8*, 108−115.
41. Wulff, K., and Herrmann, F. H. (2000) Twenty two novel mutations of the factor VII gene in factor VII deficiency, *Hum. Mutat. 15*, 489−496.
42. Giannelli, F., Green, P. M., Sommer, S. S., Lillicrap, D. P., Ludwig, M., Schwaab, R., Reitsma, P. H., Goossens, M., Yoshioka, A., and Brownlee, G. G. (1994) Haemophilia B: database of point mutations and short additions and deletions, fifth edition, 1994, *Nucleic Acids Res. 22*, 3534−3546.
43. Uprichard, J., and Perry, D. J. (2002) Factor X deficiency, *Blood Rev. 16*, 97−110.
44. Pasternak, A., Liu, X., Lin, T. Y., and Hedstrom, L. (1998) Activating a zymogen without proteolytic processing: mutation of Lys15 and Asn194 activates trypsinogen, *Biochemistry 37*, 16201−16210.
45. Braud, S., Parry, M. A., Maroun, R., Bon, C., and Wisner, A. (2000) The contribution of residues 192 and 193 to the specificity of snake venom serine proteinases, *J. Biol. Chem. 275*, 1823−1828.
46. Kang, J., Wiegand, U., and Müller-Hill, B. (1992) Identification of cDNAs encoding two novel rat pancreatic serine proteases, *Gene 110*, 181−187.
47. Huber, R., and Bennett, W. S., Jr. (1983) Functional significance of flexibility in proteins, *Biopolymers 22*, 261−279.
48. Pasternak, A., White, A., Jeffery, C. J., Medina, N., Cahoon, M., Ringe, D., and Hedstrom, L. (2001) The energetic cost of induced fit catalysis: Crystal structures of trypsinogen mutants with enhanced activity and inhibitor affinity, *Protein Sci. 10*, 1331−1342.
49. Case, A., and Stein, R. L. (2003) Mechanistic origins of the substrate selectivity of serine proteases, *Biochemistry 42*, 3335−3348.
50. Hengge, A. C., and Stein, R. L. (2004) Role of protein conformational mobility in enzyme catalysis: acylation of alpha-chymotrypsin by specific peptide substrates, *Biochemistry 43*, 742−747.

BI701454E